

Accepted Manuscript

Design and Synthesis of 1-(1-Benzothiophen-7-yl)-1*H*-Pyrazole, a Novel Series of G Protein-coupled Receptor 52 (GPR52) Agonists

Takashi Nakahata, Kazuyuki Tokumaru, Yoshiteru Ito, Naoki Ishii, Masaki Setoh, Yuji Shimizu, Toshiya Harasawa, Kazunobu Aoyama, Teruki Hamada, Masakuni Kori, Kazuyoshi Aso

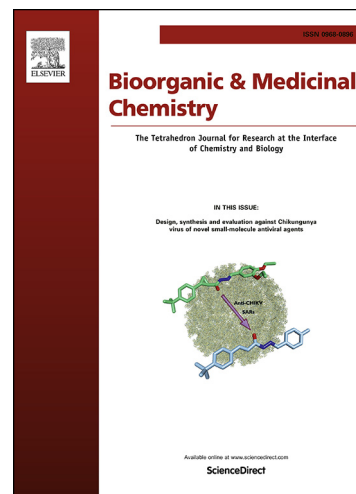
PII: S0968-0896(17)32105-3
DOI: <https://doi.org/10.1016/j.bmc.2018.02.005>
Reference: BMC 14191

To appear in: *Bioorganic & Medicinal Chemistry*

Received Date: 27 October 2017
Revised Date: 24 January 2018
Accepted Date: 5 February 2018

Please cite this article as: Nakahata, T., Tokumaru, K., Ito, Y., Ishii, N., Setoh, M., Shimizu, Y., Harasawa, T., Aoyama, K., Hamada, T., Kori, M., Aso, K., Design and Synthesis of 1-(1-Benzothiophen-7-yl)-1*H*-Pyrazole, a Novel Series of G Protein-coupled Receptor 52 (GPR52) Agonists, *Bioorganic & Medicinal Chemistry* (2018), doi: <https://doi.org/10.1016/j.bmc.2018.02.005>

This is a PDF file of an unedited manuscript that has been accepted for publication. As a service to our customers we are providing this early version of the manuscript. The manuscript will undergo copyediting, typesetting, and review of the resulting proof before it is published in its final form. Please note that during the production process errors may be discovered which could affect the content, and all legal disclaimers that apply to the journal pertain.



Design and Synthesis of 1-(1-Benzothiophen-7-yl)-1H-Pyrazole, a Novel Series of G Protein-coupled Receptor 52 (GPR52) Agonists

Takashi Nakahata ^{a,c*}, Kazuyuki Tokumaru ^a, Yoshiteru Ito ^a, Naoki Ishii ^a, Masaki Setoh ^a, Yuji Shimizu ^a, Toshiya Harasawa ^a, Kazunobu Aoyama ^{a,d}, Teruki Hamada ^{a,d}, Masakuni Kori ^b and Kazuyoshi Aso ^{a,d*}

^aPharmaceutical Research Division, Takeda Pharmaceutical Company Ltd., 26-1, Muraoka-higashi 2-chome, Fujisawa, Kanagawa 251-8555, Japan

^bPharmaceutical Sciences, Takeda Pharmaceutical Company Ltd., 17-85, Jusohonmachi-2-chome, Yodogawa-ku, Osaka 532-8686, Japan

*Corresponding authors. Tel.: +81 466 32 1126; fax: +81 466 29 4473.

E-mail: takashi.nakahata1@takeda.com (T. Nakahata).

kazuyoshi.aso@axcelead-ddp.com (K. Aso).

^cCurrent address: Cardurion Pharmaceuticals K.K., 26-1, Muraoka-Higashi 2-Chome, Fujisawa, Kanagawa 251-8555, Japan

^dCurrent address: Axcelead Drug Discovery Partners, Inc., 26-1, Muraoka-Higashi 2-Chome, Fujisawa, Kanagawa 251-0012, Japan

ABSTRACT

G-protein-coupled receptor 52 (GPR52) is classified as an orphan Gs-coupled G-protein-coupled receptor. GPR52 cancels dopamine D2 receptor signaling and activates dopamine D1/N-methyl-D-aspartate receptors via intracellular cAMP accumulation. Therefore, GPR52 agonists are expected to alleviate symptoms of psychotic disorders. A novel series of 1-(benzothiophen-7-yl)-1*H*-pyrazole as GPR52 agonists was designed and synthesized based on compound **1b**. Compound **1b** has been reported by our group as the first orally active GPR52 agonist, but high lipophilicity and poor aqueous solubility still remained as issues for candidate selection. To resolve these issues, replacement of the benzene ring at the 7-position of compound **1b** with heterocyclic rings, such as pyrazole and pyridine, was greatly expected to reduce lipophilicity to levels for which calculated logD values were lower than that of compound **1b**. While evaluating the pyrazole derivatives, introduction of a methyl substituent at the 3-position of the pyrazole ring led to increased GPR52 agonistic activity. Moreover, additional methyl substituent at the 5-position of the pyrazole and further introduction of hydroxy group to lower logD led to significant improvement of solubility while maintaining the activity. As a result, we identified 3-methyl-5-hydroxymethyl-1*H*-pyrazole derivative **17** (GPR52 EC₅₀ = 21 nM, E_{max} = 103%, logD = 2.21, Solubility at pH 6.8 = 21 µg/mL) with potent GPR52 agonistic activity and good solubility compared to compound **1b**. Furthermore, this compound **17** dose-dependently suppressed methamphetamine-induced hyperlocomotion in mice.

Key words: GPCR; GPR52 agonist; Benzothiophene; 1*H*-Pyrazole; Solubility; Methamphetamine (MAP)-induced hyperlocomotion.

Abbreviations: GPR52, G protein-coupled receptor 52; SAR, structure–activity relationship; cAMP, 3',5'-cyclic adenosine monophosphate; EC₅₀, half maximal effective concentration; MAP, methamphetamine; NMDA, *N*-methyl-D-aspartate; PK, pharmacokinetic; CHO, Chinese hamster ovary; SEM, standard error of the mean; AUC, area under the curve.

1. Introduction

G protein-coupled receptor 52 (GPR52) is an orphan Gs-coupled GPCR,¹ and a surrogate ligand of GPR52 has been reported by our research group.^{2,3} Localization of GPR52 mRNA in rat brain, which was studied by *in situ* hybridization test, indicated that GPR52 was highly expressed in the mesolimbic system and co-localized with the dopamine D2 receptors in the nucleus accumbens. GPR52 was also partially co-localized with the dopamine D1 receptors in the medial prefrontal cortex.² Moreover, GPR52 transgenic mice showed *anti*-psychiatric-like behaviors, whereas GPR52 knockout mice displayed psychosis-related behaviors.² These findings demonstrate great potential that activation of GPR52 would ameliorate the positive symptoms of schizophrenia^{4,5} by antagonizing D2 receptor signaling as well as enhancing cognitive function by activation of D1/*N*-methyl-D-aspartate (NMDA) function via intracellular cAMP accumulation. Thus, GPR52 agonists

are expected to become a novel class of antipsychotics to satisfy the unmet medical needs of the current typical and atypical agents.

The benzothiophene derivatives **1a-c** were discovered as the first GPR52 agonists in our laboratory (**Figure 1**).⁶ Recently, we also reported thiazole derivative **2** and 1,2,4-triazole derivative **3** with potent GPR52 agonistic activity as different chemotypes.^{7,8}

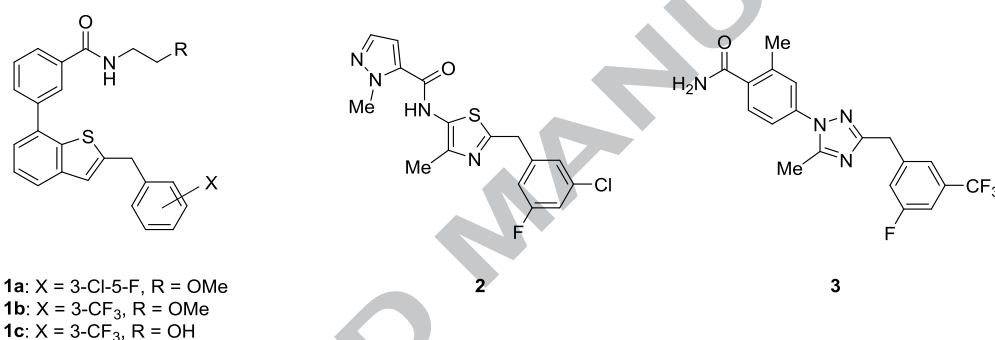


Figure 1. Reported GPR52 agonists **1a-c**, **2** and **3**.

2. Design and synthesis

2.1. Design

We previously examined impacts of a core structure on GPR52 agonistic activity,⁶ providing not only identification of the first small molecule GPR52 agonists **1a-c**, but also a key strategy to enhance GPR52 agonistic activity. Discovery of 3-(1-benzothiophen-7-yl)benzamide derivatives opened the way to the development of a novel class of antipsychotic drugs. The compound **1a** and its derivatives, however, still have some issues as drug candidates of central nervous system (CNS) in

terms of physicochemical and pharmacokinetic (PK) profiles. Especially, high lipophilicity and poor aqueous solubility of the compounds **1a** ($\log D_{\text{pH}7.4} = 7.05$, Solubility at pH 6.8 = $<0.05 \mu\text{g/mL}$), **1b** ($\log D_{\text{pH}7.4} = 7.17$, Solubility at pH 6.8 = $<0.06 \mu\text{g/mL}$), and **1c** ($\log D_{\text{pH}7.4} = 6.37$, Solubility at pH 6.8 = $0.11 \mu\text{g/mL}$) needed to be improved for drug discovery. High lipophilicity is considered as a primary reason of poor aqueous solubility and lowering of oral absorption as well as posing several toxicity issues.^{9,10,11,12} In addition, lipophilicity is one of the key structural properties that greatly affect the passive transcellular Blood-Brain Barrier (BBB) permeation of compounds. As LogD value in the range of 1-3 would be generally preferred for CNS drugs,^{13,14} we focused on lowering lipophilicity of compound **1b** for suitability as a CNS drug by replacing 7-phenyl group of **1b** with heterocyclic rings. First, we speculated that the carbonyl moiety and the benzene ring in the 2-benzyl group on benzothiophene of compound **1b** were important for GPR52 agonistic activity based on our accumulated knowledge of structure-activity relationship (SAR) around benzothiophene derivatives. In addition, the benzene ring at the 7-position of compound **1b** was considered to fill the large space as a linker that connected between the carbonyl moiety and the 2-benzylbenzothiophene moiety of compound **1b** for enhancement of the GPR52 agonistic activity. On the basis of these hypotheses, we planned introduction of heterocycle rings instead of the benzene ring at the 7-position of compound **1b**.

Introduction of heterocyclic core **B-F** as a linker in structure **A** reduced calculated logD value compared with that of compound **1b** (**Figure 2**). Among them, the pyrazole derivative **B** showed the

reduced logD value (**9**; X = OMe, logD = 4.51). We expected that the pyrazole derivative **B** could improve solubility due to its low lipophilicity. In addition, because the pyrazole derivatives have several substituent patterns at 3-, 4-, and 5-position (s), we examined SAR on the pyrazole ring. Superimposition analysis performed using MOE software¹⁵ between compound **1b** and compound **B** (**9**) indicated that the carbonyl group of compound **B** (**9**) successfully overlapped with that of the lead compound **1b** (**Figure 3**). Furthermore, the benzene ring in the 2-benzyl group on benzothiophene **1b** also overlapped with that on benzothiophene **B** (**9**). In the previous report,⁶ we reported that location of the benzene ring in the 2-benzyl group on compound **1b** would impact enhancement of GPR52 agonistic activity. Thus, pyrazole derivatives (**10-18**) with various substituent patterns were designed. The pyrazole derivatives (**11-15**) introduced a methyl group at the 3- and/or 5-position (s) on the pyrazole ring **B** (**9**) or **10** were designed to clarify the tolerability of the substituent sites for the GPR52 agonistic activity. The pyrazole derivative **16** was designed to examine regiochemistry effects of a pyrazole ring compared with compound **11**. The pyrazole derivatives **17** and **18** were designed to further lower lipophilicity, aiming at lowering logD by introducing a hydroxy group at the 3- or 5-position on the pyrazole ring. Finally, the *N*-2-methoxyethyl group and the *N*-2-hydroxyethyl group, which showed potent activity as reported in the previous paper,⁶ were selected as an amide moiety of the pyrazole derivatives (**9-18**).

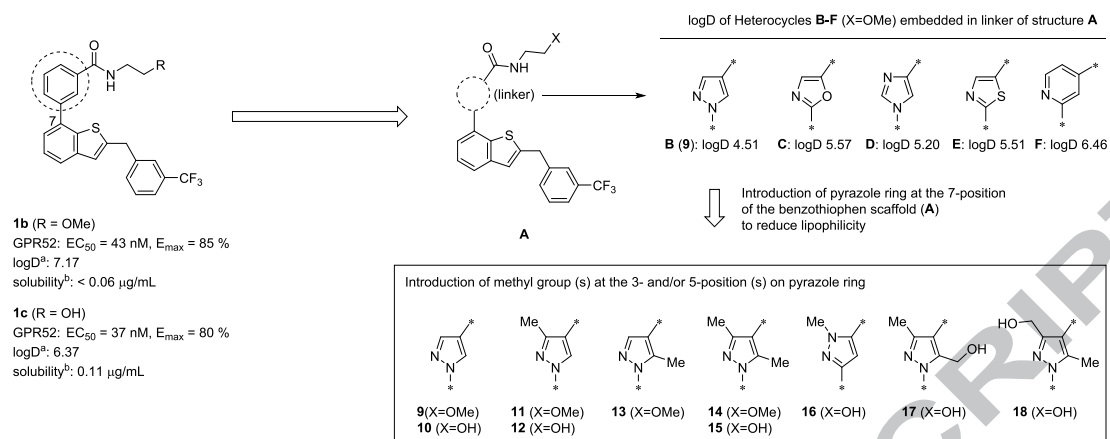


Figure 2. Design of pyrazole derivatives.

^a logD at pH7.4 was calculated using ACD/LogD, version 12.

^b The second fluid for the disintegration test is described in the Japanese Pharmacopoeia 15th edition (pH 6.8).

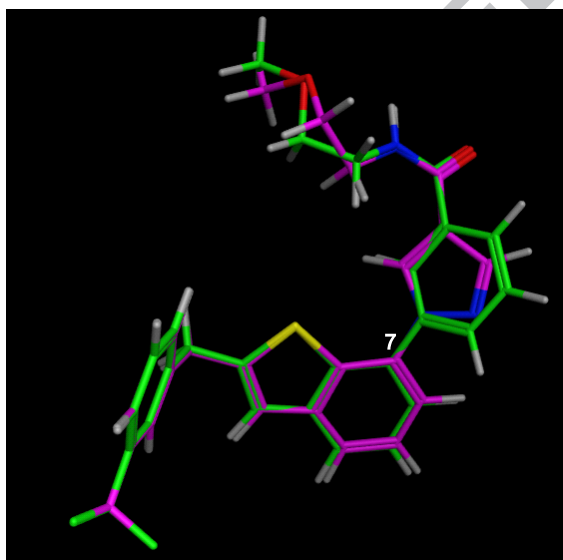
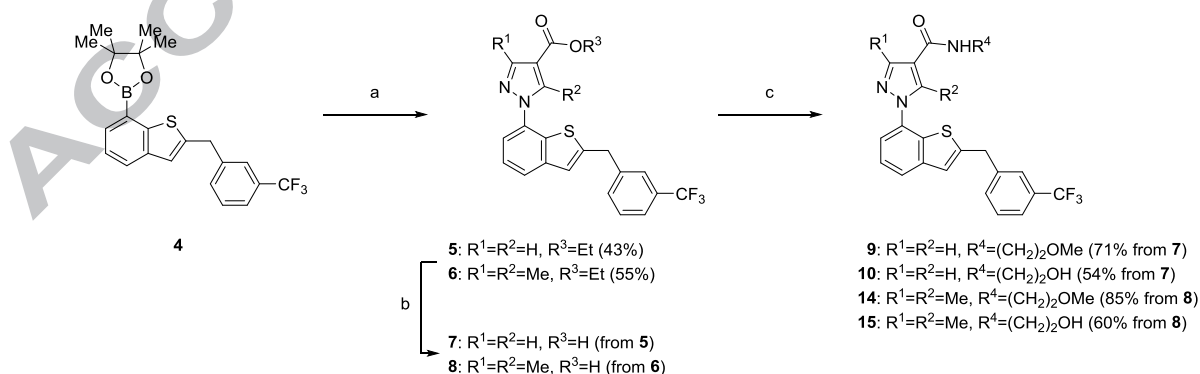


Figure 3. Superimposition model of compounds **1b** (lime green) and **B = 9** (magenta). This image was generated using MOE 2013.08.

Herein, we describe discovery of a novel series of 1-(benzothiophen-7-yl)-1*H*-pyrazole as GPR52 agonists and their synthesis and physicochemical parameters. Biological and pharmacological effects of the representative compounds are also discussed.

2.2. Chemistry

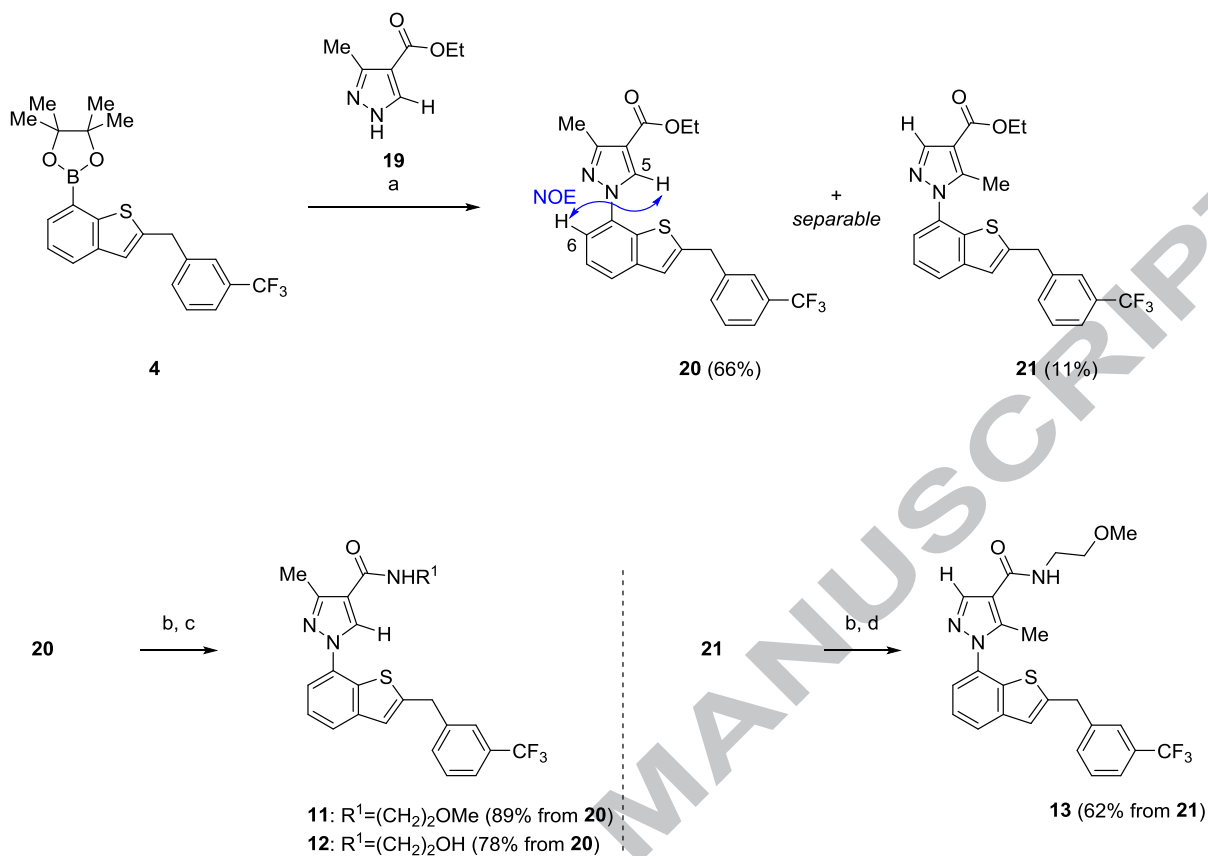
The designed pyrazole compounds **9**, **10**, **14**, and **15** were synthesized by a common synthetic route (**Scheme 1**). Preparation of starting boronic ester **4** as a key intermediate is described in **Scheme 5**. Copper-promoted coupling reaction¹⁶ of the boronic ester **4** with ethyl *1H*-pyrazole-4-carboxylate or ethyl 3,5-dimethyl-*1H*-pyrazole-4-carboxylate afforded pyrazole esters **5** and **6**, respectively. Basic hydrolysis of the esters **5** and **6** gave corresponding carboxylic acids **7** and **8**, followed by condensation with amines (R^4NH_2) to afford the desired amide derivatives **9**, **10**, **14** and **15**.



Scheme 1^a

^a Reagents and conditions: (a) pyrazoles, Cu(OAc)₂, pyridine, 50 °C; (b) NaOH aq., THF-EtOH, 80 °C; (c) R⁴NH₂, HOBt, EDCI, DMF.

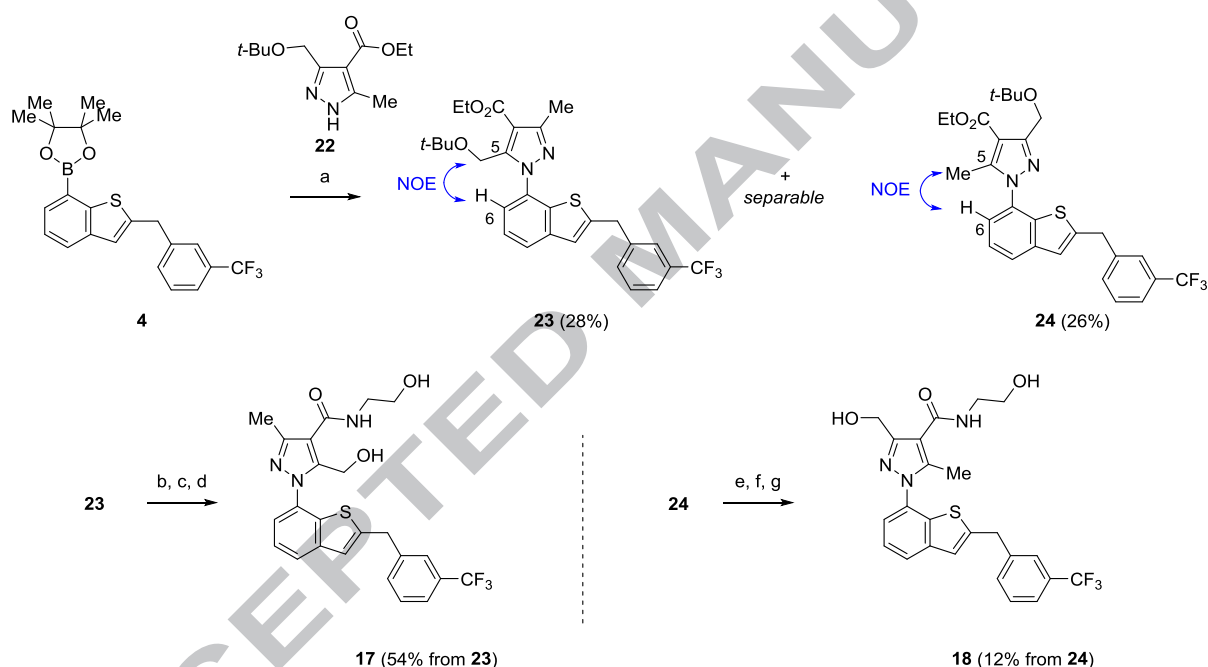
The boronic ester **4** was treated with commercially available ethyl 3-methyl-1*H*-pyrazole-4-carboxylate **19** to afford esters **20** and **21** (*ca.*6:1) as a regioisomeric mixture, which were separated by silica gel column chromatography (**Scheme 2**). The methyl-substituted position on pyrazole ring of the ester **20** was determined by two-dimensional (2D) nuclear magnetic resonance (NMR). **In compound 20, a nuclear overhauser effect (NOE) was observed between the proton at C6-position of the benzothiophene core and the proton at C5-position of the pyrazole ring.** After hydrolysis of the esters **20** and **21** under basic condition, corresponding carboxylic acids were condensed with 2-methoxyethyl amine or 2-aminoethanol to afford the desired pyrazol derivatives **11** and **12**. The minor regioisomer **21** was converted into the only methoxyethyl amide **13**.

Scheme 2^a

^a Reagents and conditions: (a) Cu(OAc)₂, pyridine., 50 °C; (b) NaOH aq., THF-EtOH, 80 °C; (c) R¹NH₂, HOBt, EDCI, *i*-Pr₂NEt, DMF; (d) MeO(CH₂)₂NH₂, HOBt, EDCI, DMF.

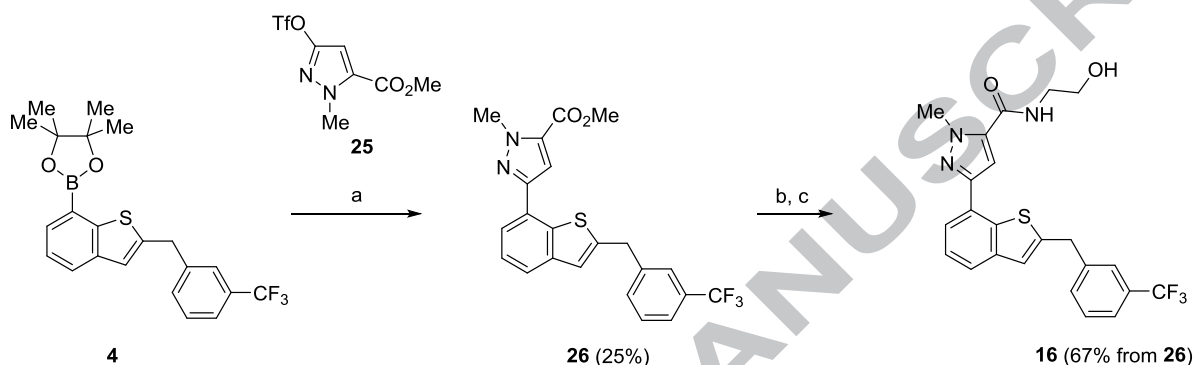
Synthesis of hydroxymethyl pyrazole derivatives **17** and **18** is shown in **Scheme 3**. Copper-promoted coupling of the boronic ester **4** with reported pyrazole derivative **22**¹⁷ gave esters **23** and **24** (*ca.*1:1) as a regioisomeric mixture. After separation of the regioisomers **23** and **24** by silica gel column chromatography, the substituted position of *tert*-butoxymethyl on the pyrazole ring of the esters **23** and **24** was also determined by 2D NMR. **In compound 23, NOE was observed between the proton at C6-position of the benzothiophene core and the methylene protons at C5-position**

of the pyrazole ring. On the other hand, NOE was observed in compound **24** between the proton at C6-position of the benzothiophene core and the methyl group at C5-position of the pyrazole ring. After removal of the *tert*-butyl group under acidic condition and basic hydrolysis of the ethyl esters of **23** and **24**, corresponding carboxylic acids were condensed with 2-aminoethanol to afford the desired pyrazol derivatives **17** and **18**.

Scheme 3^a

^a Reagents and conditions: (a) Cu(OAc)₂, pyridine., 50 °C; (b) 4 M HCl/EtOAc; (c) NaOH aq., THF-EtOH, 80 °C; (d) H₂N(CH₂)₂OH, HOBt, EDCI, DMF; (e) 4 M HCl/EtOAc; (f) NaOH aq., THF-EtOH, 80 °C; (g) H₂N(CH₂)₂OH, HOBt, EDCI, DMF.

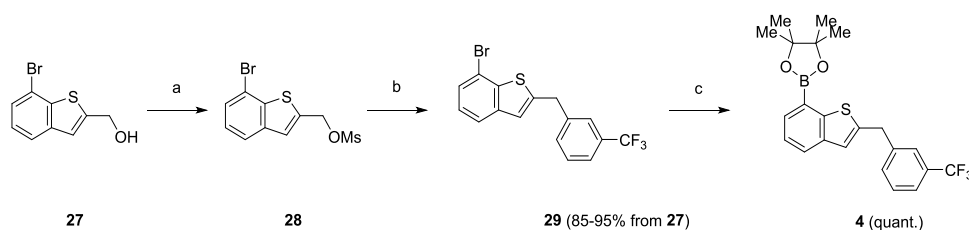
N-Methyl pyrazole ester **26** was prepared by Suzuki-Miyaura coupling¹⁸ of the boronic ester **4** with the reported triflate **25**.¹⁹ Basic hydrolysis of the ester **26** gave the corresponding carboxylic acid, which was condensed with 2-aminoethanol to afford the pyrazole derivative **16** (**Scheme 4**).



Scheme 4^a

^a Reagents and conditions: (a) Pd(PPh₃)₄, Na₂CO₃, DMF, 95 °C, 25%; (b) NaOH aq., THF-EtOH, 80 °C; (c) NH₂(CH₂)₂OH, HOBT, EDCI, *i*-Pr₂NEt, DMF.

Preparation of the key intermediate boronic ester **4** described above is depicted in **Scheme 5**. The boronic ester **4** was prepared by concise methods. Hydroxymethyl benzothiophene **27** was treated with methanesulfonyl chloride to afford mesylate **28**. Suzuki-Miyaura coupling reaction of the mesylate **28** with 3-trifluoromethylphenylboronic acid regioselectively gave bromide **29** without other coupling adducts. Palladium-catalyzed cross-coupling reaction of the bromide **29** with Bis(pinacolato)diboron afforded boronic ester **4**.



Scheme 5^a

^a Reagents and conditions: (a) Et₃N, MsCl, THF, 0 °C to rt; (b) *m*-CF₃PhB(OH)₂, Cs₂CO₃, PdCl₂(dppf)·CH₂Cl₂, THF-H₂O, 60 °C; (c) (pin-B)₂, PdCl₂(dppf)·CH₂Cl₂, AcOK, DMF, 85 °C.

3. Biological results and discussion

3.1. In vitro assay

GPR52 agonistic activity of the synthesized compounds **9-18** was determined from the cAMP production by using human GPR52 expressed on Chinese hamster ovary (CHO) cell lines. The EC₅₀ values were calculated from the concentration-activity curve of each agonist producing 50% response of 1 μM of the reference compound (*N*-(2-hydroxyethyl)-3-[2-[3-(trifluoromethyl)benzyl]-1-benzofuran-4-yl]benzamide)⁶ (**Table 1**).

The 3,5-unsubstituted pyrazole derivatives **9** and **10**, and the 5-methyl pyrazole derivative **13** showed moderate GPR52 agonistic activities with EC₅₀ values of 62 nM, 87 nM, and 62 nM, respectively. The 5-methyl group on the pyrazole ring (**13**) did not affect the enhancement of the GPR52 agonistic activity compared with compound **9**. On the other hand, introduction of a methyl group at the 3-position on the pyrazole ring (**11** and **12**) remarkably increased GPR52 agonistic activity (EC₅₀ = 9.6 nM, E_{max} = 89% for **11**; 5.7 nM, E_{max} = 102% for **12**) compared with the 3,5-

unsubstituted pyrazole derivatives **9** ($EC_{50} = 62$ nM, $E_{max} = 81\%$) and **10** ($EC_{50} = 87$ nM, $E_{max} = 73\%$). Furthermore, the 3,5-dimethyl pyrazole derivatives **14** and **15** ($EC_{50} = 17$ nM, $E_{max} = 104\%$ for **14**; 15 nM, $E_{max} = 110\%$ for **15**) also showed a higher potency than the 3,5-unsubstituted pyrazole derivatives (**9** and **10**). Based on these results, introduction of the 3-methyl group on the pyrazole ring (**11** and **14**) clearly increased the potency compared with the 3,5-unsubstituted pyrazole derivative (**9**) and the 5-methyl pyrazole derivative (**13**). To examine effect of the 3-methyl group on the pyrazole ring, we conducted superimposition studies of compounds **11**, **14**, and **1b** using the MNDO-PM3 (MOPAC version 7.01) method in MOE (**Figure 4**). The 3-methyl group of compounds **11** and **14** successfully occupied the hydrophobic space located around the 7-benzene ring of **1b**. These data suggested that introduction of the 3-methyl group into the pyrazole ring filled the spatial gap of ring size observed between the pyrazole ring of compound **9** and the benzene ring of compound **1b**. On the other hand, the 5-methyl group of the 3,5-dimethylpyrazole derivative **14** would have no impact on the GPR52 agonistic activity, because the 5-methylpyrazole derivative **13** was as potent as the 3,5-unsubstituted pyrazole derivative **9**. The 5-methyl group of compound **14** was located outside the 7-benzene ring of **1b**, as observed in **Figure 4**.

As a result of SAR study of pyrazole derivatives (**9-15**), the *N*-2-hydroxyethyl group as an amide moiety showed a potent GPR52 agonistic activity and also decreased logD value by 0.81 compared with the *N*-2-methoxyethyl group. Therefore, the *N*-2-hydroxyethyl group was selected as an amide moiety for further investigation. The GPR52 agonistic activity of compound **16** ($EC_{50} = 45$ nM) was

diminished compared with compound **12** ($EC_{50} = 5.2$ nM). The methyl group on the polar nitrogen atom of the pyrazole ring in compound **16** could be intolerable for the GPR52 agonistic activity. Hydrophilic substituent effect at the 3-position or the 5-position on the pyrazole ring in compound **15** was examined by introduction of a hydroxy group. The GPR52 agonistic activity of the 5-hydroxymethyl-3-methyl pyrazole derivative **17** ($EC_{50} = 21$ nM, $E_{max} = 103\%$) was as potent as that of **15**, whereas the 3-hydroxymethyl-5-methyl pyrazole derivative **18** ($EC_{50} = 146$ nM) showed weaker GPR52 agonistic activity than compounds **15** and **17**. The hydroxy group at the 5-position on the pyrazole ring **15** was fully tolerated for the GPR52 agonistic activity, while 3-hydroxymethyl group on the pyrazole ring **18** was intolerable.

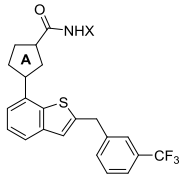
3.2. Solubility

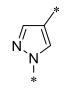
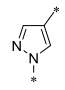
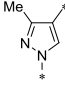
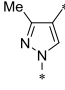
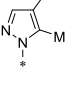
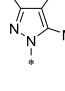
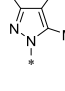
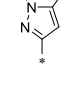
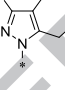
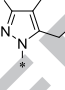
Aqueous Solubility of the synthesized compounds **9-18** is also shown in **Table 1**. Compounds **9-12** and **16** showed poor solubility, whereas the 5-methyl pyrazole derivative **13** (solubility at pH 6.8 = 1.3 $\mu\text{g/mL}$) showed better solubility than the 3,5-unsubstituted pyrazole derivative **9** (solubility at pH 6.8 = <0.08 $\mu\text{g/mL}$). Furthermore, the 3,5-dimethyl pyrazole derivatives **14** and **15** (solubility at pH 6.8 = 2.9 $\mu\text{g/mL}$ and 12 $\mu\text{g/mL}$, respectively) provided much better solubility than the 3,5-unsubstituted pyrazole derivatives **9** and **10** (solubility at pH 6.8 = <0.09 $\mu\text{g/mL}$) or the 3-methyl pyrazole derivatives **11** and **12** (solubility at pH 6.8 = <0.1 $\mu\text{g/mL}$ and <0.1 $\mu\text{g/mL}$, respectively). Improvement of the solubility of compounds **13**, **14**, and **15** was considered to be caused by reducing

their logD values. However, solubility of the 5-methyl pyrazole derivative **13** was greatly improved compared with compound **11** even though the logD value of both compounds is 4.29. In addition, the 3-methyl pyrazole derivative **12** showed poorer solubility than compounds **13** and **14**, although the logD value of compound **12** (logD = 3.48) was lower than those of compounds **13** and **14** (logD = 4.08). These results suggested that the methyl group at the 5-position on the pyrazole ring in compounds **13**, **14**, and **15** plays an important role to improve the solubility independently of the logD value as a lipophilic parameter.

We performed global minimum conformational analyses of compounds **11** and **14** in MOE to confirm an effect of the methyl group at the 5-position on the pyrazole ring of compound **14** (**Figure 5**). The dihedral angle between benzothiophene core of compound **11** and the 3-methyl pyrazole ring at 7-position was nearly planar (3.7°), as shown in **Figure 5** (left image), while the dihedral angle between benzothiophene core of compound **14** and the 3,5-dimethyl pyrazole ring at 7-position was 30.6° , because of the steric hindrance by the 5-methyl group on the pyrazole ring, as shown in **Figure 5** (right image). These analyses suggested that introduction of the 5-methyl group on the pyrazole ring of compound **14** caused disruption of molecular planarity and improvement of the solubility in addition to the decrease in logD value.²⁰

Solubility of the compounds **17** and **18** (logD = 2.21 and 2.21, respectively) with a hydroxyl group at 3-position or 5-position in the pyrazole ring was increased because of lower logD values than for compound **15** (logD = 3.27).

Table 1. GPR52 agonistic activities and physicochemical properties of pyrazole derivatives.


Compound	Ring A	X	Human GPR52 ^a		Solubility ^b ($\mu\text{g/ml}$) at pH 6.8	logD ^c
			EC ₅₀ (nM)	E _{max} (%)		
9		CH ₂ CH ₂ OMe	62 (49-80)	81 (76-88)	<0.08	4.51
10		CH ₂ CH ₂ OH	87 (47-163)	73 (61-85)	<0.09	3.70
11		CH ₂ CH ₂ OMe	9.6 (8.2-11)	89 (86-92)	<0.1	4.29
12		CH ₂ CH ₂ OH	5.2 (4.7-5.7)	102 (100-103)	<0.1	3.48
13		CH ₂ CH ₂ OMe	62 (52-73)	84 (81-88)	1.3	4.29
14		CH ₂ CH ₂ OMe	17 (14-19)	104 (101-108)	2.9	4.08
15		CH ₂ CH ₂ OH	15 (13-17)	110 (107-113)	12	3.27
16		CH ₂ CH ₂ OH	45 (28-73)	110 (100-122)	<0.08	6.94
17		CH ₂ CH ₂ OH	21 (15-28)	103 (96-109)	21	2.21
18		CH ₂ CH ₂ OH	146 (121-176)	96 (91-101)	18	2.21

^a EC₅₀ values are derived from the mean curves of the experiments (n =2-4). Numbers in parentheses represent the 95% confidence interval.

^b The second fluid for the disintegration test is described in the Japanese Pharmacopoeia 15th edition (pH 6.8).

^c logD at pH 7.4 was calculated using ACD/LogD, version 12.

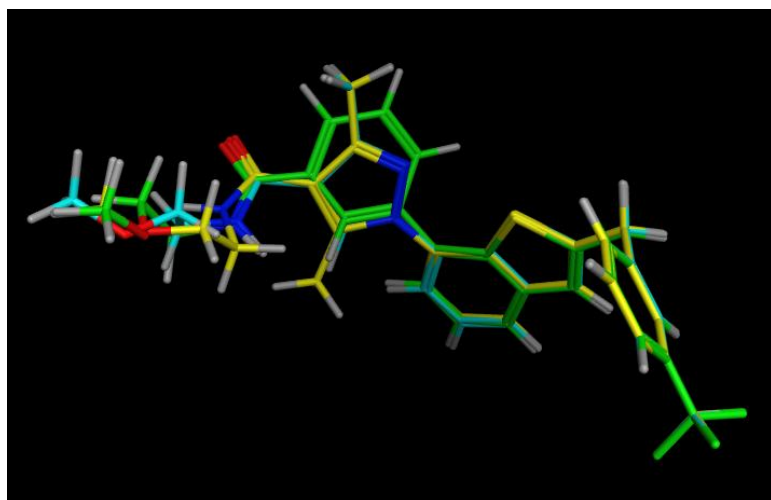


Figure 4. Superimposition model of compounds **1b** (lime green), **11** (cyan), and **14** (yellow). This image was generated using MOE 2013.08.

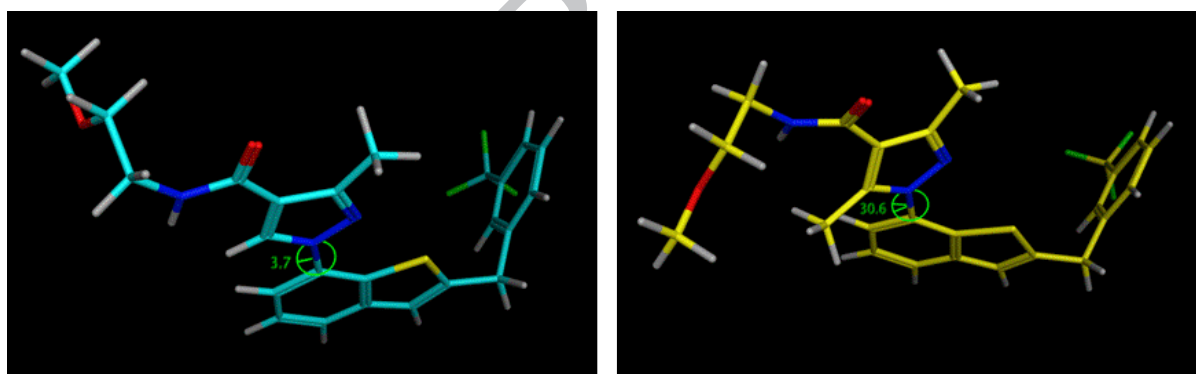


Figure 5. Minimized structures **11** (left image) and **14** (right image). These images were generated using MOE 2013.08.

3.3. Pharmacokinetic Profiles

Compound **17** showed highly potent GPR52 agonistic activity, good solubility, and acceptable logD values in the range 1-3 favored for CNS drugs^{13,14} among synthesized pyrazole derivatives (**9-**

18, Table 1), and therefore compound **17** was selected for further PK evaluations. It was found that compound **17** possessed good oral absorption ($C_{max} = 83.0$ ng/mL; $T_{max} = 1.7$ h; $AUC_{0-8h} = 405.5$ ng·h/mL; F (bioavailability) = 29.9%, mouse cassette dosing at 0.1 mg/kg, iv and 1 mg/kg, p.o.) and the plasma protein binding value in mice at 1 μ M concentration was 98% (**Table 2**). In addition to its moderate PK profile in mice, the multidrug resistance (MDR) efflux ratio of compound **17** was 1.7. These results led to expectation that compound **17** would be a non-substrate of p-glycoprotein1 and show a high brain penetration as oral administration.

In our previous study, we reported that compound **1a** ($EC_{50} = 30$ nM, $E_{max} = 79.8\%$), used for *in vivo* pharmacological evaluation, possessed oral PK profile [$C_{max} = 108.1$ ng/mL; $T_{max} = 2$ h; $AUC_{0-8h} = 613.7$ ng·h/mL; F (bioavailability) = 73%, mouse cassette dosing at 0.1 mg/kg, iv and 1 mg/kg, po] and good brain penetration (brain/plasma AUC ratio B/P = 0.94, in mice after oral administration of 30 mg/kg).⁶ As compared to compound **1a**, GPR52 agonistic activity and PK profile of compound **17** were similar to compound **1a**, whereas the solubility of compound **17** was much higher than that of compound **1a**. Moreover, MDR efflux ratio of compound **17** was suitable for use as an *in vivo* tool compound. Based on these results, compound **17** was found to be suitable as a biological *in vivo* tool compound.

Table 2. Pharmacokinetic profile in mice of compound **17**.

compound	C _{max} ^{a,b} (ng/mL)	T _{max} ^{a,c} (h)	AUC _{po} ^{a,d} (ng*h/mL)	Cl _{total} ^{a,e} (mL/h/kg)	F ^{a,f} (%)	MDR Efflux ratio
17	83.0	1.7	405.5	747	29.9	1.7

^a Mice cassette dosing. ICR mice (n=3). Dose: 0.1 mg/kg, i.v.; 1 mg/kg, p.o. Data are presented as averages for 3 mice.

^b Maximum drug concentration.

^c Time of maximum drug concentration observed.

^d Area under the curve from 0 to 8 h.

^e Clearance.

^f Bioavailability.

3.4. MAP-induced hyperlocomotion

Thus, compound **17**, with acceptable PK profile, was evaluated for antipsychotic efficacy by methamphetamine (MAP)-induced hyperlocomotion²¹ test in mice. Compound **17** dose-dependently suppressed MAP-induced hyperlocomotion at 10 and 30 mg/kg after oral administration (**Figure 6**). Haloperidol, currently employed clinically as an antipsychotic, also suppressed MAP-induced hyperlocomotion, at 0.3 mg/kg. In addition, no nonspecific effect, such as sedation, general malaise, or compound toxicity, was observed during a 60-minute period after pretreatment of compound **17**. These data indicate that compound **17** has a potent antipsychotic-like effect in mice.

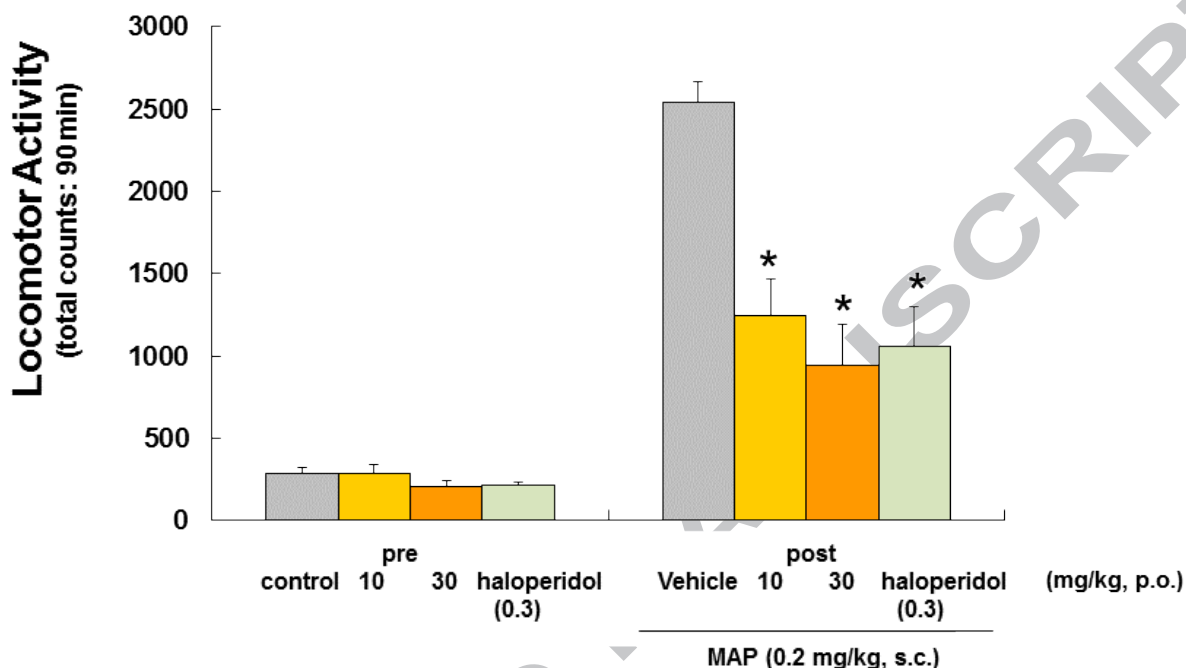


Figure 6. Dose-dependent inhibition of MAP-induced hyperlocomotion by compound **17** in mice. Mice were administered compound **17** (10, 30 mg/kg, p.o.) and haloperidol (0.3 mg/kg, p.o.) and placed in activity chambers for 60 min. After this period, MAP (2 mg/kg, s.c.) was injected and measurement was started. Data are expressed as mean \pm S.E.M. ($n = 6-7$ per group). Data were analyzed by Williams' test, $*P < 0.025$ versus the control group treated with vehicle and MAP.

4. Conclusions

A novel series of 1-(benzothiophen-7-yl)-1*H*-pyrazole GPR52 agonists was designed and synthesized to improve high lipophilicity and poor solubility of the compound **1b**. The newly designed pyrazole derivatives (**9-18**) were efficiently synthesized by synthetic routes using Suzuki-

Miyaura coupling and Chan-Lam-Evans coupling conditions as key reactions. In the evaluation of these pyrazole derivatives, we found introduction of the methyl substituent at the 3-position of the pyrazole ring led to enhancement of the GPR52 agonistic activity. Moreover, substituents at the 5-position on the pyrazole ring would play an important role to improve the solubility. As a result, we identified 3-methyl-5-hydroxymethyl-1*H*-pyrazole derivative **17** with highly potent GPR52 agonistic activity ($EC_{50} = 21$ nM, $E_{max} = 103\%$), good solubility (21 $\mu\text{g/mL}$ at pH 6.8), and acceptable bioavailability ($F = 29.9\%$). Furthermore, this compound **17** also suppressed methamphetamine-induced hyperlocomotion in mice after oral administration (10 and 30 mg/kg, p.o.). These results indicate that the newly designed pyrazole GPR52 agonists have potential as a next generation antipsychotics.

5. Experimental protocols

5.1.1. General

The proton nuclear magnetic resonance (^1H NMR) spectra were determined on a Bruker AVANCE II (300 MHz) or Varian INOVA- 400 (400 MHz) instruments. Chemical shifts for ^1H NMR were reported in parts per million (ppm) downfield from tetramethylsilane (δ) as the internal standard in deuterated solvent and coupling constants (J) are in Hertz (Hz). The following abbreviations are used for spin multiplicity: s = singlet, d = doublet, t = triplet, q = quartet, m = multiplet and br = broad. Elemental analyses were carried out by Takeda Analytical Research

Laboratories, Ltd. In the following experimental, melting points were determined on a Büchi B-545 and were uncorrected. Analytical thin layer chromatography (TLC) was performed on silica gel 60 F254 plates (Merck) or NH TLC plate (Fuji Silysia Chemical Ltd.). Column chromatography was carried out on a silica gel column (Chromatorex[®] NH-DM1020, 100–200 mesh, Fuji Silysia chemical) or on Purif-Pack (SI / 60 IM or NH / 60 IM, Fuji Silysia Chemical, Ltd.). Liquid chromatography-mass spectrometry (LC/ MS) analysis was performed on the following methods; (A) an Agilent 1200, equipped with a L-column2 ODS (3.0 × 50 mm I.D., 3 μ m-particle size, CERI, Japan), eluting with 5 mM ammonium acetate (AcONH₄) in ultrapure water/acetonitrile = 90/10 (Mobile phase A), and 5 mM AcONH₄ in ultrapure water/acetonitrile = 10/90 (Mobile phase B), using the following elution gradient of 5% B to 90% B over 0.9 min followed by 90% B isocratic over 1.1 min at a flow rate of 1.5 mL/min (detection at 220 nm or 254 nm). MS spectra were recorded using an Agilent 6130 with electrospray ionization. (B) a Shimadzu LC-20AD, equipped with a L-column2 ODS (3.0 × 50 mm I.D., 3 μ m-particle size, CERI, Japan), eluting with 5 mM AcONH₄ in ultrapure water/acetonitrile = 90/10 (Mobile phase A), and 5 mM AcONH₄ in ultrapure water/acetonitrile = 10/90 (Mobile phase B), using the following elution gradient of 5% B to 90% B over 0.9 min followed by 90% B isocratic over 1.1 min at a flow rate of 1.5 mL/min (detection at 220 nm or 254 nm). MS spectra were recorded using a Shimadzu LCMS-2020 with electrospray ionization. (C) a Shimadzu LC- 20AD, equipped with a L-column2 ODS (3.0 × 50 mm I.D., 3 μ m-particle size, CERI, Japan), eluting with 0.05% TFA in ultrapure water (Mobile phase A), and

0.05% TFA in acetonitrile (Mobile phase B), using the following elution gradient of 5% B to 90% B over 0.9 min followed by 90% B isocratic over 1.1 min at a flow rate of 1.5 mL/min (detection at 220 nm). MS spectra were recorded using a Shimadzu LCMS-2020 with electrospray ionization. (D) a Waters 2795, equipped with a L-column2 ODS (3.0 × 50 mm I.D., 3 μm particle size, CERI, Japan), eluting with 0.05% TFA in ultrapure water (Mobile phase A), and 0.05% TFA in acetonitrile (Mobile phase B), using the following elution gradient of 5% B to 90% B over 2 min followed by 90% B isocratic over 1.5 min at a flow rate of 1.2 mL/min (detection at 220 nm or 254 nm). MS spectra were recorded using a Waters ZQ2000 with electrospray ionization. Preparative LC was performed on a Waters 2525 separations module (L-column2 ODS (20 × 150 mm I.D., CERI, Japan); 0.1% TFA in distilled water/acetonitrile gradient; MS spectra were recorded using a Waters ZQ2000 with electrospray ionization. The purities of all compounds tested in biological systems were assessed as being >95% using analytical high-performance liquid chromatography (HPLC). Purity data were collected by a HPLC with Corona CAD (Charged Aerosol Detector) or photo diode array detector. The column was a Capcell Pak C18AQ (50 mm × 3.0 mm I.D., Shiseido, Japan) or L-column 2 ODS (30 mm × 2.0 mm I.D., CERI, Japan) with a temperature of 50 °C and a flow rate of 0.5 mL/min. Mobile phase A and B under a neutral condition were a mixture of 50 mmol/L AcONH₄, water and acetonitrile (1:8:1, v/v/v) and a mixture of 50 mmol/L AcONH₄ and acetonitrile (1:9, v/v), respectively. The ratio of mobile phase B was increased linearly from 5% to 95% over 3 min, 95% over the next 1 min. Mobile phase A and B under an acidic condition were a mixture of 0.2% formic

acid in 10 mmol/L ammonium formate and 0.2% formic acid in acetonitrile, respectively. The ratio of mobile phase B was increased linearly from 14% to 86% over 3 min, 86% over the next 1 min. All commercially available solvents and reagents were used without further purification. Yields were not optimized. Abbreviations: (pin-B)₂, bis(pinacolato) diboron; Pd(Ph₃P)₄, tetrakis(triphenylphosphine)-palladium(0); PdCl₂(dppf)-CH₂Cl₂, dichloro [1,10-bis(diphenylphosphino)ferrocene] palladium(II) CH₂Cl₂ adduct; Na₂CO₃, sodium carbonate; NaHCO₃, sodium hydrogen carbonate; NaOH, sodium hydroxide; K₂CO₃, potassium carbonate; Cs₂CO₃, cesium carbonate; AcOK, potassium acetate; MgSO₄, magnesium sulfate; TFA, trifluoroacetic acid; NH₄Cl, ammonium chloride; MsCl, methanesulfonyl chloride; EDCI, 1-(3-dimethylaminopropyl)-3-ethylcarbodiimide hydrochloride; HOBt, 1-hydroxybenzotriazole; *i*-Pr₂NEt, di-isopropylethylamine; Et₃N, triethylamine; HCl, hydrochloric acid; DMF, *N,N*-dimethylformamide; DMSO, dimethylsulfoxide; EtOAc, ethyl acetate; MeOH, methyl alcohol; EtOH, ethyl alcohol; THF, tetrahydrofuran.

5.1.2. Ethyl 1-(2-(3-(trifluoromethyl)benzyl)-1-benzothiophen-7-yl)-1*H*-pyrazole-4-carboxylate (**5**)

To a solution of 4,4,5,5-tetramethyl-2-(2-(3-(trifluoromethyl)benzyl)-1-benzothiophen-7-yl)-1,3,2-dioxaborolane (**4**) (1.25 g, 3.0 mmol) and ethyl 1*H*-pyrazole-4-carboxylate (840 mg, 6.0 mmol) in pyridine (10 mL) was added Cupric acetate, monohydrate (1.19 g, 6.0 mmol) at room temperature. The mixture was stirred at 50 °C under a dry atmosphere (CaCl₂ tube) overnight. The mixture was quenched with water at room temperature and extracted with EtOAc. The organic layer was

separated, washed with 1 M HCl and brine, dried over MgSO₄ and concentrated in vacuo. The residue was purified by column chromatography (silica gel, eluted with 0% - 25% EtOAc in hexane) to give **5** (557 mg, 43%) as colorless crystals.

¹H-NMR (300 MHz, CDCl₃) δ: 1.39 (3H, t, *J* = 7.1 Hz), 4.29 (2H, s), 4.36 (2H, q, *J* = 7.1 Hz), 7.08–7.11 (1H, m), 7.38–7.57 (6H, m), 7.68 (1H, dd, *J* = 6.6, 2.2 Hz), 8.18 (1H, s), 8.50 (1H, s).

5.1.3. Ethyl 3,5-dimethyl-1-(2-(3-(trifluoromethyl)benzyl)-1-benzothiophen-7-yl)-1*H*-pyrazole-4-carboxylate (**6**)

Compound **6** was prepared in a manner similar to that desired for **5** in 55% yield.

¹H-NMR (300 MHz, CDCl₃) δ: 1.39 (3H, t, *J* = 7.1 Hz), 2.46 (3H, s), 2.52 (3H, s), 4.26 (2H, s), 4.34 (2H, q, *J* = 7.1 Hz), 7.08 (1H, t, *J* = 1.1 Hz), 7.20 (1H, dd, *J* = 7.6, 1.0 Hz), 7.37–7.55 (5H, m), 7.73 (1H, dd, *J* = 8.0, 1.1 Hz).

5.1.4. *N*-(2-methoxyethyl)-1-(2-(3-(trifluoromethyl)benzyl)-1-benzothiophen-7-yl)-1*H*-pyrazole-4-carboxamide (**9**)

To a solution of ethyl 1-(2-(3-(trifluoromethyl)benzyl)benzo[b]thiophen-7-yl)-1*H*-pyrazole-4-carboxylate (**5**) (557 mg, 1.29 mmol) in THF (5 ml)/EtOH (5.00 ml) was added 8 M NaOH aq. (0.324 ml, 2.59 mmol) at room temperature. The mixture was stirred at 80 °C under a dry atmosphere (CaCl₂ tube) overnight. 6 M HCl was added to bring the pH of the solution to 2-3 and extracted with

EtOAc. The organic layer was separated, washed with water and brine, dried over MgSO_4 and concentrated in vacuo. This product was subjected to the next reaction without further purification. To a solution of 1-(2-(3-(trifluoromethyl)benzyl)benzo[b]thiophen-7-yl)-1*H*-pyrazole-4-carboxylic acid (**7**) (200 mg, 0.50 mmol), WSC (HCl) (191 mg, 0.99 mmol) and *i*Pr₂EtN (0.260 ml, 1.49 mmol) in DMF (5 ml) was added HOBt (Anhydrous) (134 mg, 0.99 mmol) at room temperature. After being stirred at room temperature for 10 min, 2-methoxyethanamine (74.7 mg, 0.99 mmol) was added to the reaction mixture. The mixture was stirred at room temperature under N₂ overnight. The mixture was quenched with sat. NH₄Cl aq. at room temperature and extracted with EtOAc. The organic layer was separated, washed with water and brine, dried over MgSO_4 and concentrated in vacuo. The residue was purified by column chromatography (silica gel, eluted with 0% - 60% EtOAc in hexane and 0% - 5% MeOH in EtOAc) and crystallized from EtOAc-hexane to give **9** (420 mg, 71%) as colorless crystals.

¹H-NMR (300 MHz, CDCl₃) δ : 3.41 (3 H, s), 3.53 - 3.69 (4 H, m), 4.29 (2 H, s), 6.22 (1 H, br s), 7.08 - 7.11 (1 H, m), 7.40 - 7.58 (6 H, m), 7.66 - 7.70 (1 H, m), 8.02 (1 H, d, $J = 0.8$ Hz), 8.47 (1 H, d, $J = 0.8$ Hz). ¹³C NMR (75 MHz, CDCl₃) δ : 36.4, 39.2, 58.8, 71.2, 114.6, 120.2, 122.0, 122.3, 123.7 (q, $J_{\text{C-F}} = 3.7$ Hz), 124.9, 125.4 (q, $J_{\text{C-F}} = 3.7$ Hz), 127.6 (q, $J_{\text{C-F}} = 270$ Hz), 129.2, 129.3, 131.0 (d, $J_{\text{C-F}} = 32$ Hz), 131.2, 132.1, 134.2, 138.7, 140.0, 142.6, 146.5, 162.1. mp: 157 – 159 °C. MS (ESI+) $m/z = 460.1$ [M+H]⁺. Chemical purity 100%.

5.1.5. *N*-(2-methoxyethyl)-3,5-dimethyl-1-(2-(3-(trifluoromethyl)benzyl)-1-benzothiophen-7-yl)-
1*H*-pyrazole-4-carboxamide (**14**)

Compound **14** was prepared from **6** in a manner similar to that described for **9** in 85% yield. ¹H-NMR (300 MHz, CDCl₃) δ: 2.43 (3 H, s), 2.50 (3 H, s), 3.40 (3 H, s), 3.53 - 3.68 (4 H, m), 4.25 (2 H, s), 6.06 - 6.16 (1 H, m), 7.05 - 7.09 (1 H, m), 7.18 (1 H, dd, *J* = 7.7, 0.8 Hz), 7.35 - 7.54 (5 H, m), 7.71 (1 H, dd, *J* = 8.0, 0.8 Hz). ¹³C NMR (75 MHz, CDCl₃) δ: 11.9, 14.1, 36.6, 39.0, 58.8, 71.3, 114.6, 121.4, 122.1, 123.4, 123.8 (q, *J*_{C-F} = 3.9 Hz), 124.7, 125.5 (q, *J*_{C-F} = 3.9 Hz), 127.6 (q, *J*_{C-F} = 272.9 Hz), 129.2, 131.0 (d, *J*_{C-F} = 31.9 Hz), 132.2, 133.0, 137.0, 139.9, 142.0, 142.8, 145.6, 147.6, 164.5. MS (ESI+) *m/z* = 488.1 [M+H]⁺. Chemical purity 100%.

5.1.6. *N*-(2-hydroxyethyl)-1-(2-(3-(trifluoromethyl)benzyl)-1-benzothiophen-7-yl)-1*H*-pyrazole-4-
carboxamide (**10**)

Compound **10** was prepared in a manner similar to that desired for **9** in 54% yield.

¹H-NMR (300 MHz, CDCl₃) δ: 3.27 - 3.37 (2 H, m), 3.45 - 3.59 (2 H, m), 4.33 - 4.47 (2 H, m), 4.69 - 4.82 (1 H, m), 7.28 - 7.38 (1 H, m), 7.41 - 7.83 (7 H, m), 8.16 - 8.35 (2 H, m), 8.95 - 9.07 (1 H, m). mp: 226 - 228 °C. MS (ESI+) *m/z* = 446.1 [M+H]⁺.

5.1.7. *N*-(2-hydroxyethyl)-3,5-dimethyl-1-(2-(3-(trifluoromethyl)benzyl)-1-benzothiophen-7-yl)-
1*H*-pyrazole-4-carboxamide (**15**)

Compound **15** was prepared from **6** in a manner similar to that desired for **9** in 60% yield.

$^1\text{H-NMR}$ (300 MHz, CDCl_3) δ : 2.44 (3H, s), 2.52 (3H, s), 2.63 (1H, t, $J = 4.9$ Hz), 3.59–3.68 (2H, m), 3.81–3.89 (2H, m), 4.26 (2H, s), 6.15 (1H, br s), 7.09 (1H, t, $J = 1.1$ Hz), 7.19 (1H, dd, $J = 7.5$, 0.8 Hz), 7.38–7.55 (5H, m), 7.74 (1H, dd, $J = 7.9$, 1.1 Hz). mp: 137–139 °C. MS (ESI+) $m/z = 474.1$ $[\text{M}+\text{H}]^+$. Chemical purity 100%. Anal. Calcd for $\text{C}_{24}\text{H}_{22}\text{N}_3\text{O}_2\text{SF}_3$: C, 60.88; H, 4.68; N, 8.87. Found: C, 60.81; H, 4.70; N, 8.87.

5.1.8. Ethyl 3-methyl-1-(2-(3-(trifluoromethyl)benzyl)-1-benzothiophen-7-yl)-1*H*-pyrazole-4-carboxylate (**20**)

and ethyl 5-methyl-1-(2-(3-(trifluoromethyl)benzyl)-1-benzothiophen-7-yl)-1*H*-pyrazole-4-carboxylate (**21**)

To a solution of 4,4,5,5-tetramethyl-2-(2-(3-(trifluoromethyl)benzyl)-1-benzothiophen-7-yl)-1,3,2-dioxaborolane (**4**) (1.25 g, 3.0 mmol) and ethyl 3-methyl-1*H*-pyrazole-4-carboxylate (554 mg, 3.6 mmol) in pyridine (15 mL) was added Cupric acetate, monohydrate (300 mg, 1.5 mmol) at room temperature. The mixture was stirred at 50 °C under a dry atmosphere (CaCl_2 tube) overnight. The mixture was quenched with water at room temperature and extracted with EtOAc. The organic layer was separated, washed with 1 M HCl aq. and brine, dried over MgSO_4 and concentrated in vacuo. The residue was purified by column chromatography (silica gel, eluted with 0% - 35% EtOAc in hexane) to give **20** (884 mg, 66%) as colorless crystals and **21** (150 mg, 11%) as a brown oil.

Compound **20**: $^1\text{H-NMR}$ (300 MHz, CDCl_3) δ : 1.38 (3H, t, $J = 7.2$ Hz), 2.51 (3H, s), 4.26 (2H, s), 4.34 (2H, q, $J = 6.9$ Hz), 7.10 (1H, s), 7.23 (1H, dd, $J = 7.6, 1.1$ Hz), 7.39–7.55 (5H, m), 7.76 (1H, dd, $J = 8.0, 1.1$ Hz), 8.10 (1H, s).

Compound **21**: $^1\text{H-NMR}$ (300 MHz, CDCl_3) δ : 1.38 (3H, t, $J = 7.2$ Hz), 2.60 (3H, s), 4.29 (2H, s), 4.33 (2H, q, $J = 6.9$ Hz), 7.06–7.08 (1H, m), 7.35–7.68 (7H, m), 8.44 (1H, s).

5.1.9. *N*-(2-methoxyethyl)-3-methyl-1-(2-(3-(trifluoromethyl)benzyl)-1-benzothiophen-7-yl)-1*H*-pyrazole-4-carboxamide (**11**)

Compound **11** was prepared from **20** in a manner similar to that desired for **9** in 89% yield.

$^1\text{H-NMR}$ (300 MHz, CDCl_3) δ : 2.61 (3 H, s), 3.39 (3 H, s), 3.51 - 3.68 (4 H, m), 4.28 (2 H, s), 6.26 (1 H, t, $J = 4.5$ Hz), 7.06 (1 H, t, $J = 1.1$ Hz), 7.33 - 7.67 (7 H, m), 8.34 (1 H, s). mp: 97 - 100 °C. MS (ESI+) $m/z = 474.1$ $[\text{M}+\text{H}]^+$. Chemical purity 97%.

5.1.10. *N*-(2-hydroxyethyl)-3-methyl-1-(2-(3-(trifluoromethyl)benzyl)-1-benzothiophen-7-yl)-1*H*-pyrazole-4-carboxamide (**12**)

Compound **12** was prepared from **20** in a manner similar to that desired for **9** in 78% yield.

$^1\text{H-NMR}$ (300 MHz, CDCl_3) δ : 2.47 (1 H, t, $J = 4.9$ Hz), 2.62 (3 H, s), 3.58 - 3.67 (2 H, m), 3.80 - 3.89 (2 H, m), 4.29 (2 H, s), 6.24 (1 H, br s), 7.06 - 7.10 (1 H, m), 7.35 - 7.68 (7 H, m), 8.35 (1 H, s). mp: 122-124 °C. MS (ESI+) $m/z = 460.1$ $[\text{M}+\text{H}]^+$. Chemical purity 100%.

5.1.11. *N*-(2-methoxyethyl)-5-methyl-1-(2-(3-(trifluoromethyl)benzyl)-1-benzothiophen-7-yl)-1*H*-pyrazole-4-carboxamide (**13**)

Compound **13** was prepared from **21** in a manner similar to that desired for **9** in 62% yield.

¹H-NMR (300 MHz, CDCl₃) δ: 2.53 (3H, s), 3.40 (3H, s), 3.51–3.70 (4H, m), 4.25 (2H, s), 6.23 (1H, t, *J* = 4.5 Hz), 7.10 (1H, s), 7.19–7.24 (1H, m), 7.37–7.57 (5H, m), 7.73–7.78 (1H, m), 7.88 (1H, s).

MS (ESI+) *m/z* = 474.1 [M+H]⁺. Chemical purity 100%.

5.1.12. Ethyl 5-(tert-butoxymethyl)-3-methyl-1-(2-(3-(trifluoromethyl)benzyl)-1-benzothiophen-7-yl)-1*H*-pyrazole-4-carboxylate (**23**)
and ethyl 3-(tert-butoxymethyl)-5-methyl-1-(2-(3-(trifluoromethyl)benzyl)-1-benzothiophen-7-yl)-1*H*-pyrazole-4-carboxylate (**24**)

To a solution of 4,4,5,5-tetramethyl-2-(2-(3-(trifluoromethyl)benzyl)-1-benzothiophen-7-yl)-1,3,2-dioxaborolane (**4**) (3.12 g, 7.45 mmol) and ethyl 5-(tert-butoxymethyl)-3-methyl-1*H*-pyrazole-4-carboxylate (1.79 g, 7.45 mmol) in pyridine (15 mL) was added Cupric acetate, monohydrate (300 mg, 1.5 mmol) at room temperature. The mixture was stirred at 55 °C under a dry atmosphere (CaCl₂ tube) overnight. The mixture was concentrated in vacuo. The residue was purified by column chromatography (silica gel, eluted with 0% - 25% EtOAc in hexane) to give **23** (1.11 g, 28%) as colorless crystals and **24** (1.03 g, 26%) as a brown oil.

Compound **23**: $^1\text{H-NMR}$ (300 MHz, CDCl_3) δ : 1.08 (9H, s), 1.35–1.43 (3H, m), 2.53 (3H, s), 4.25 (2H, s), 4.35 (2H, q, $J = 7.1$ Hz), 4.56 (2H, s), 7.08 (1H, s), 7.34–7.63 (6H, m), 7.73 (1H, d, $J = 8.0$ Hz).

Compound **24**: $^1\text{H-NMR}$ (300 MHz, CDCl_3) δ : 1.31 (9H, s), 1.39 (3H, t, $J = 7.1$ Hz), 2.45 (3H, s), 4.25 (2H, s), 4.35 (2H, q, $J = 7.1$ Hz), 4.72 (2H, s), 7.08 (1H, s), 7.21 (1H, d, $J = 7.7$ Hz), 7.36–7.47 (3H, m), 7.48–7.55 (2H, m), 7.73 (1H, d, $J = 8.0$ Hz).

5.1.13. *N*-(2-hydroxyethyl)-5-(hydroxymethyl)-3-methyl-1-(2-(3-(trifluoromethyl)benzyl)-1-benzothiophen-7-yl)-1*H*-pyrazole-4-carboxamide (**17**)

The mixture of ethyl 5-(tert-butoxymethyl)-3-methyl-1-(2-(3-(trifluoromethyl)benzyl)-1-benzothiophen-7-yl)-1*H*-pyrazole-4-carboxylate (**23**) (1.11 g, 2.09 mmol) and 4 M HCl/EtOAc (15 mL) was stirred at room temperature under N_2 overnight. The mixture concentrated in vacuo. This product was subjected to the next reaction without further purification. To a solution of the residue in THF (10 ml)/EtOH (10 ml) was added 8 M NaOH aq. (0.522 ml, 4.18 mmol) at room temperature. The mixture was stirred at 80 °C under a dry atmosphere (CaCl_2 tube) overnight. 6 M HCl was added to bring the pH of the solution to 2-3 and extracted with EtOAc. The organic layer was separated, washed with water and brine, dried over MgSO_4 and concentrated in vacuo. This product was subjected to the next reaction without further purification. To a solution of the corresponding carboxylic acid, WSC (HCl) (801 mg, 4.18 mmol) and *i*Pr₂EtN (1.09 ml, 6.27 mmol) in DMF (5 ml)

was added HOBt (Anhydrous) (564 mg, 4.18 mmol) at room temperature. After being stirred at room temperature for 10 min, 2-methoxyethanamine (255 mg, 4.18 mmol) was added to the reaction mixture. The mixture was stirred at room temperature under N₂ overnight. The mixture was quenched with sat. NH₄Cl aq. at room temperature and extracted with EtOAc. The organic layer was separated, washed with water and brine, dried over MgSO₄ and concentrated in vacuo. The residue was purified by column chromatography (silica gel, eluted with 0% - 60% EtOAc in hexane and 0% - 5% MeOH in EtOAc) and crystallized from EtOAc-hexane to give **17** (551 mg, 54%) as a white solids. ¹H-NMR (300 MHz, CDCl₃) δ: 2.39 (1H, br s), 2.57 (3H, s), 3.61–3.71 (2H, m), 3.86 (2H, br s), 4.26 (2H, s), 4.60 (2H, d, *J* = 6.4 Hz), 4.98 (1H, t, *J* = 7.0 Hz), 6.62 (1H, br s), 7.09 (1H, s), 7.25–7.31 (1H, m), 7.38–7.47 (3H, m), 7.49–7.55 (2H, m), 7.75 (1H, d, *J* = 7.9 Hz). ¹³C NMR (75 MHz, CDCl₃) δ: 14.2, 36.6, 42.2, 54.9, 62.1, 115.2, 121.3, 122.2, 123.8, 123.8 (q, *J*_{C-F} = 3.9 Hz), 124.9, 125.5 (q, *J*_{C-F} = 3.9 Hz), 127.6 (q, *J*_{C-F} = 272 Hz), 129.2, 131.0 (q, *J*_{C-F} = 32.5 Hz), 132.2, 132.3, 136.6, 139.8, 142.1, 145.7, 146.4, 147.6, 165.9. mp: 112–113 °C. MS (ESI+) *m/z* = 490.1 [M+H]⁺. Chemical purity 97%. Anal. Calcd for C₂₄H₂₂N₃O₃SF₃·1.3H₂O: C, 56.20; H, 4.83; N, 8.19. Found: C, 55.99; H, 4.49; N, 8.34.

5.1.14. *N*-(2-hydroxyethyl)-3-(hydroxymethyl)-5-methyl-1-(2-(3-(trifluoromethyl)benzyl)-1-benzothiophen-7-yl)-1*H*-pyrazole-4-carboxamide (**18**)

Compound **18** was prepared from **24** in a manner similar to that desired for **17** in 12% yield.

$^1\text{H-NMR}$ (300 MHz, CDCl_3) δ : 2.48 (3H, s), 3.08 (1H, br s), 3.32 (1H, br s), 3.55–3.67 (2H, m), 3.78–3.90 (2H, m), 4.26 (2H, s), 4.78–4.91 (2H, m), 7.06–7.59 (7H, m), 7.76 (1H, d, $J = 8.2$ Hz), 7.96 (1H, br s). $^{13}\text{C NMR}$ (75 MHz, CDCl_3) δ : 11.8, 36.6, 42.6, 58.5, 62.9, 114.6, 121.7, 122.2, 123.9, 123.9 (q, $J_{\text{C-F}} = 3.9$ Hz), 124.9, 125.5 (q, $J_{\text{C-F}} = 3.9$ Hz), 127.6 (q, $J_{\text{C-F}} = 272$ Hz), 129.2, 131.0 (q, $J_{\text{C-F}} = 31.9$ Hz), 132.2, 132.5, 137.0, 139.8, 142.0, 144.6, 145.7, 150.3, 165.6. MS (ESI+) $m/z = 490.2$ $[\text{M}+\text{H}]^+$. Chemical purity 91%.

5.1.15. Methyl 1-methyl-3-(2-(3-(trifluoromethyl)benzyl)-1-benzothiophen-7-yl)-1*H*-pyrazole-5-carboxylate (**26**)

A mixture of **4** (0.80 g, 1.92 mmol), methyl 1-methyl-3-(((trifluoromethyl)sulfonyl)oxy)-1*H*-pyrazole-5-carboxylate (**25**) (0.37 g, 1.28 mmol), and $\text{Pd}(\text{PPh}_3)_4$ (150 mg, 0.13 mmol) in 2 M Na_2CO_3 aq. (1.28 mL)-DMF (10 mL) was stirred at 95 °C under N_2 atmosphere overnight. Then the reaction mixture was concentrated under reduced pressure, diluted with water, and extracted with EtOAc. The extract was washed with brine, then dried over MgSO_4 and concentrated in vacuo. The residue was purified by column chromatography (silica gel, eluted with 0% - 10% EtOAc in hexane) to give **26** (140 mg, 25%) as colorless crystals.

$^1\text{H-NMR}$ (300 MHz, CDCl_3) δ : 3.93 (3H, s), 4.29 (3H, s), 4.32 (2H, s), 7.08 (1H, s), 7.31 (1H, s), 7.36–7.54 (4H, m), 7.58 (1H, s), 7.64–7.71 (2H, m).

5.1.16. *N*-(2-hydroxyethyl)-1-methyl-3-(2-(3-(trifluoromethyl)benzyl)-1-benzothiophen-7-yl)-1*H*-pyrazole-5-carboxamide (**16**)

Compound **16** was prepared from **26** in a manner similar to that desired for **9** in 67% yield.

¹H-NMR (300 MHz, CDCl₃) δ: 2.14 (1 H, t, J = 4.9 Hz), 3.63 (2 H, q, J = 5.3 Hz), 3.86 (2 H, q, J = 4.9 Hz), 4.27 (3 H, s), 4.32 (2 H, s), 6.51 (1 H, brs), 6.99 (1 H, s), 7.08 (1 H, s), 7.35-7.47 (2 H, m), 7.48-7.55 (2 H, m), 7.58 (1 H, s), 7.66 (2 H, dd, J = 12.1, 7.2 Hz). ¹³C NMR (75 MHz, CDCl₃) δ: 36.5, 39.7, 42.2, 62.0, 103.9, 121.8, 122.1, 122.9, 123.6 (q, J_{C-F} = 3.9 Hz), 124.5, 125.5 (q, J_{C-F} = 3.9 Hz), 127.7 (q, J_{C-F} = 272 Hz), 126.8, 129.1, 130.9 (q, J_{C-F} = 32.5 Hz), 132.2, 136.1, 136.2, 140.5, 141.2, 145.0, 148.5, 160.6. mp: 127 - 128 °C. MS (ESI+) m/z = 460.1 [M+H]⁺. Chemical purity 100%.

5.2. Biology

5.2.1. cAMP assay

The intracellular cAMP level was determined by using an Alphascreen cAMP Detection Kit (PerkinElmer), by following the manufacturer's instructions. CHO cells expressing human GPR52 (10,000 cells) were incubated with test compounds for 30 min at 37°C in 30 μL/well of assay buffer (Hanks' balanced salt solution (HBSS) containing 5 mM HEPES (2-[4-(2-hydroxyethyl)-1-piperazinyl]ethanesulfonic acid) (pH7.6), 0.5% BSA (bovine serum albumin), 100 μM IBMX (3-isobutyl-1-methylxanthine), and 100 μM Ro20-1724 (4-(3-Butoxy-4-methoxybenzyl)-imidazolidin-

2-one). Then, 10 μL /well of 0.1 U/ μL anti cAMP acceptor beads (PerkinElmer) and 10 μL /well of 0.1 U/ μL biotinylated cAMP donor beads (PerkinElmer) were added and incubated overnight at room temperature. cAMP concentrations were determined by measuring AlphaScreen signal with Envision (PerkinElmer).

5.2.2. Solubility determination

Small volumes of the compound DMSO solutions were added to the aqueous buffer (pH 6.8). After incubation, precipitates were separated from by filtration through a filter plate. The filtrates were analyzed for compound in solution by HPLC analysis.

5.2.3. Pharmacokinetic analysis in mice cassette dosing

Test compounds were administered intravenously (0.1 mg/kg) or orally (1 mg/kg) by cassette dosing to male ICR mouse. After administration, blood samples were collected and centrifuged to obtain the plasma fraction. The plasma samples were deproteinized followed by centrifugation. The compound concentrations in the supernatant were measured by LC/MS/MS.

5.2.4. Phychostimulants-induced hyperlocomotion test

Male ICR mice (7-8 weeks) were used for all experiments. The locomotor activity in mice was measured using locomotor activity monitors, MDC-LT (Brain Science Idea Co., Ltd). Mice were individually placed in transparent polycarbonate cages (30 × 40 × 20 cm). After habituation for 60 min, compound **17** (10 and 30 mg/kg, p.o.) and haloperidol (0.3 mg/kg, p.o.) were administered. MAP (2 mg/kg, s.c.) was injected 60 min after the drug treatment. Activity counts were monitored for 150 min after administration of **17** and haloperidol.

6. Acknowledgements

We acknowledge Hiroyuki Ota and Keiji Nishiyama for discussions regarding *in vivo* MAP-induced hyperlocomotion test, Hideki Matsui for discussions regarding *in vitro* assay, Teruaki Okuda for DMPK analysis, Eiji Kimura and members of the GPR52 agonist project for expertise in chemistry, providing helpful information and discussion.

7. References

1. Sawzdargo et al., *Molecular Brain Research*, 1999, *64*: 193-198. M. Sawzdargo, T. Nguyena, D.K. Leea, K.R. Lynchb, R. Chenga, H.H.Q. Hengc, S.R. Georgea, B.F. O'Dowda. Identification and cloning of three novel human G protein-coupled receptor genes GPR52, PsiGPR53 and GPR55: GPR55 is extensively expressed in human brain *Brain Res. Mol Brain Res.* 1999;64:193–198. [http://dx.doi.org/10.1016/S0169-328X\(98\)00277-0](http://dx.doi.org/10.1016/S0169-328X(98)00277-0)

2. H. Komatsu, M. Maruyama, S. Yao, T. Shinohara, K. Sakuma, S. Imaichi, T. Chikatsu, K. Kuniyeda, F. K. Siu, L. S. Peng, K. Zhuo, L. S. Mun, T. M. Han, Y. Matsumoto, T. Hashimoto, N. Miyajima, Y. Itoh, K. Ogi, Y. Habata, M. Mori, Anatomical transcriptome of G protein-coupled receptors leads to the identification of a novel therapeutic candidate GPR52 for psychiatric disorders. *PLoS ONE*. (2014);9:e90134. <http://dx.doi.org/10.1371/journal.pone.0090134>.
3. H. Komatsu. Novel therapeutic GPCRs for psychiatric disorders. *Int J Mol Sci*. (2015);16:14109–14121. <http://dx.doi.org/10.3390/ijms160614109>.
4. G.K. Thaker, W.T.Jr. Carpenter. Advances in schizophrenia. *Nat. Med.*, **2001**, 7, 667-671.
5. M.B. First, A.Ct. Tasman. *In DSM-IV-TR Mental Disorders: Diagnosis, Etology and Treatment*; Wiley: Chichester, U. K., **2004**, 639–701.
6. M. Setoh, N. Ishii, M. Kono, Y. Miyanoana, E. Shiraishi, T. Harasawa, H. Ota, T. Odani, N. Kanzaki, K. Aoyama, T. Hamada, M. Kori. *J. Med. Chem.*, **2014**, 57 (12), 226–5237.
7. E. Kimura, Y. Imaeda T. Wakabayashi, et al. Design and synthesis of 2-benzyl-1,3-thiazole derivatives as a novel class of G protein-coupled receptor 52 (GPR52) agonists 247th ACS National Meeting & Exposition Dallas, TX, United States, March 16–20, 2014; MEDI-96.
8. K. Tokumar, Y. Ito, I. Nomura, T. Nakahata, Y. Shimizu, E. Kurimoto, K. Aoyama, K. Aso. Design, synthesis, and pharmacological evaluation of 4-azolyl-benzamide derivatives as novel GPR52 agonists. *Bioorg. Med. Chem.* **2017**, 25, 3098-3115. <https://doi.org/10.1016/j.bmc.2017.03.064>

9. A. Avdeef. Physicochemical profiling (solubility, permeability and charge state). *Curr Top Med Chem.* **2001**, *1*, 277-351.
10. P.D. Leeson, B. Springthorpe. The influence of drug-like concepts on decision-making in medicinal chemistry. *Nat. Rev. Drug Discov.* **2007**, *6*, 881-890.
11. J.U. Peters, P. Schnider, P. Mattei, M. Kansy. Pharmacological promiscuity: dependence on compound properties and target specificity in a set of recent Roche compounds. *Chem. Med. Chem.* **2009**, *4*, 680-686.
12. J. D. Hughes, J. Blagg, D.A. Price, S. Bailey, G.A. DeCrescenzo, R.V. Devraj, E. Ellsworth, Y.M. Fobian, M.E. Gibbs, R.W. Gilles, N. Greene, E. Huang, T.-K. Burke, J. Loesel, T. Wager, L. Whiteley, Y. Zhang. Physicochemical drug properties associated with in vivo toxicological outcomes. *Bioorg. Med. Chem. Lett.* **2008**, *18*, 4872-4875.
<https://doi.org/10.1016/j.bmcl.2008.07.071>
13. H. Pajouhesh, G.R. Lenz. Medicinal Chemical Properties of Successful Central Nervous System Drugs. *NeuroRx.* **2005**, *2*, 541-553. <https://doi.org/10.1602/neurorx.2.4.541>
14. M.J. Waring. Lipophilicity in drug discovery. *Expert Opin. Drug Discov.* **2010**, *5* (3), 235-248.
<http://dx.doi.org/10.1517/17460441003605098>
15. MOE, version 2013.08; CCG: Montreal, Quebec, Canada, **2013**.

16. D.M.T. Chan, K.L. Monaco, R.-P. Wang. New N- and O-arylations with phenylboronic acids and cupric acetate. *Tetrahedron Lett.* **1998**, 39, 2933-2936. [https://doi.org/10.1016/S0040-4039\(98\)00503-6](https://doi.org/10.1016/S0040-4039(98)00503-6)
17. D.L. Walmsley, M.J. Drysdale, C.J. Northfield, C. Fromont. WO2006134318 A1, **2006**.
18. N. Miyaura, A. Suzuki. Palladium-catalyzed cross-coupling reactions of organoboron compounds. *Chemical Reviews*, **1995**, 95, 2457. <http://pubs.acs.org/doi/pdf/10.1021/cr00039a007>
19. M.M. Claffey, S.W. Goldstein. WO2007034278 A2, **2007**.
20. M. Ishikawa, Y. Hashimoto. Improvement in Aqueous Solubility in Small Molecule Drug Discovery Programs by Disruption of Molecular Planarity and Symmetry. *J. Med. Chem.* **2011**, 54, 1539–1554. <http://pubs.acs.org/doi/abs/10.1021/jm101356p>
21. Y. Suzuki, T. Funakoshi, S. Chaki, N. Kawashima, S. Ogawa, T. Kumagai, A. Nakazato, T. Komurasaki, S. Okuyama. In vitro and in vivo pharmacological profile of 4-(4-fluorobenzylidene)-1-[2-[5-(4-fluorophenyl)-1H-pyrazol-4-yl] ethyl] piperidine (NRA0161). *Life Sci.* **2002**; 71, 2603-15. [https://doi.org/10.1016/S0024-3205\(02\)02085-4](https://doi.org/10.1016/S0024-3205(02)02085-4)

Design and Synthesis of 1-(1-Benzothiophen-7-yl)-1H-Pyrazole, a Novel Series of G Protein-coupled Receptor 52 (GPR52) Agonists

Takashi Nakahata ^{a,c*}, Kazuyuki Tokumaru ^a, Yoshiteru Ito ^a, Naoki Ishii ^a, Masaki Setoh ^a, Yuji Shimizu ^a, Toshiya Harasawa ^a, Kazunobu Aoyama ^{a,d}, Teruki Hamada ^{a,d}, Masakuni Kori ^b and Kazuyoshi Aso ^{a,d*}

^a*Pharmaceutical Research Division, Takeda Pharmaceutical Company Ltd., 26-1, Muraoka-higashi 2-chome, Fujisawa, Kanagawa 251-8555, Japan*

^b*Pharmaceutical Sciences, Takeda Pharmaceutical Company Ltd., 17-85, Jusohonmachi-2-chome, Yodogawa-ku, Osaka 532-8686, Japan*

*Corresponding authors. Tel.: +81 466 32 1126; fax: +81 466 29 4473.

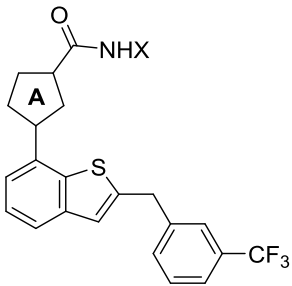
E-mail: takashi.nakahata1@takeda.com (T. Nakahata).

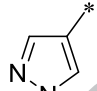

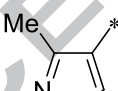
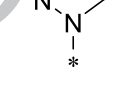
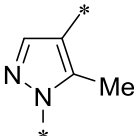
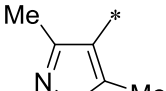
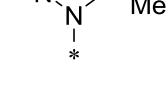
kazuyoshi.aso@axcelead-ddp.com (K. Aso).

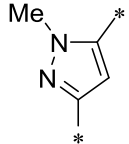
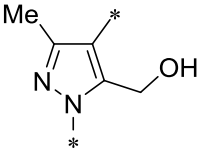
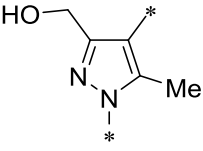
^cCurrent address: Cardurion Pharmaceuticals K.K., 26-1, Muraoka-Higashi 2-Chome, Fujisawa, Kanagawa 251-8555, Japan

^dCurrent address: Axcelead Drug Discovery Partners, Inc., 26-1, Muraoka-Higashi 2-Chome, Fujisawa, Kanagawa 251-0012, Japan

Table 1. GPR52 agonistic activities and physicochemical properties of pyrazole derivatives.



Compound	Ring A	X	Human GPR52 ^a		Solubility ^b ($\mu\text{g/mL}$) at pH 6.8	logD ^c
			EC ₅₀ (nM)	Emax (%)		
9		CH ₂ CH ₂ OMe	62 (49-80)	81 (76-88)	<0.08	4.51
10		CH ₂ CH ₂ OH	87 (47-163)	73 (61-85)	<0.09	3.70
11		CH ₂ CH ₂ OMe	9.6 (8.2-11)	89 (86-92)	<0.1	4.29
12		CH ₂ CH ₂ OH	5.2 (4.7-5.7)	102 (100-103)	<0.1	3.48
13		CH ₂ CH ₂ OMe	62 (52-73)	84 (81-88)	1.3	4.29
14		CH ₂ CH ₂ OMe	17 (14-19)	104 (101-108)	2.9	4.08
15		CH ₂ CH ₂ OH	15 (13-17)	110 (107-113)	12	3.27

16		CH ₂ CH ₂ OH	45 (28-73)	110 (100-122)	<0.08	6.94
17		CH ₂ CH ₂ OH	21 (15-28)	103 (96-109)	21	2.21
18		CH ₂ CH ₂ OH	146 (121-176)	96 (91-101)	18	2.21

^a EC₅₀ values are derived from the mean curves of the experiments (n =2-4). Numbers in parentheses represent the 95% confidence interval.

^b The second fluid for the disintegration test is described in the Japanese Pharmacopoeia 15th edition (pH 6.8).

^c logD at pH 7.4 was calculated using ACD/LogD, version 12.

Table 2. Pharmacokinetic profile in mice of compound **17**.

Compound	C _{max} ^{a,b} (ng/mL)	T _{max} ^{a,c} (h)	AUC _{po} ^{a,d} (ng*h/mL)	CL _{total} ^{a,e} (mL/h/kg)	F ^{a,f} (%)	MDR Efflux ratio
17	83.0	1.7	405.5	747	29.9	1.7

^a Mice cassette dosing. ICR mice (n=3). Dose: 0.1 mg/kg, i.v.; 1 mg/kg, p.o. Data are presented as averages for 3 mice.

^b Maximum drug concentration.

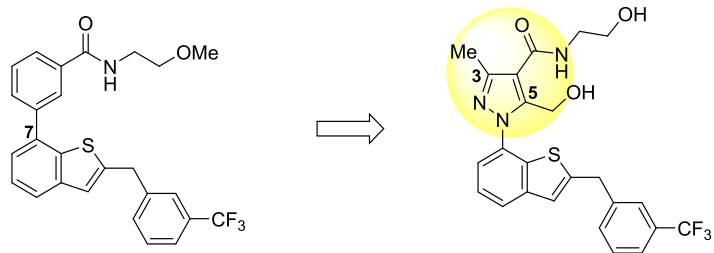
^c Time of maximum drug concentration observed.

^d Area under the curve from 0 to 8 h.

^e Clearance.

^f Bioavailability.

ACCEPTED MANUSCRIPT



1b: $EC_{50} = 43$ nM, $E_{max} = 85\%$
logD: 7.17
solubility at pH 6.8: < 0.06 $\mu\text{g/mL}$

17: $EC_{50} = 21$ nM, $E_{max} = 103\%$
logD: 2.21
solubility at pH 6.8: 21 $\mu\text{g/mL}$

ACCEPTED MANUSCRIPT